# INTEGRATED TRAFFIC CONTROL FOR FREEWAYS USING VARIABLE SPEED LIMITS AND LANE CHANGE CONTROL ACTIONS


**Vasileios Markantonakis, Corresponding Author**
Dynamic Systems and Simulation Laboratory,
School of Production Engineering & Management,
Technical University of Crete,
73100 Chania, Greece
Tel: +30 28210-37421; Email: vmarkantonakis@dssl.tuc.gr

**Dimitrios Ilias Skoufoulas**
Dynamic Systems and Simulation Laboratory,
School of Production Engineering & Management,
Technical University of Crete,
73100 Chania, Greece
Tel: +30 28210-37421; Email: dskoufoulas@isc.tuc.gr

**Ioannis Papamichail**
Dynamic Systems and Simulation Laboratory,
School of Production Engineering & Management,
Technical University of Crete,
73100 Chania, Greece
Tel: +30 28210-37422; Email: ipapa@dssl.tuc.gr

**Markos Papageorgiou**
Dynamic Systems and Simulation Laboratory,
School of Production Engineering & Management,
Technical University of Crete,
73100 Chania, Greece
Tel: +30 28210-37240; Email: markos@dssl.tuc.gr



Word Count: 5856 words text = 5856 words
Submission Date: August 1, 2018
Revision Date: November 14, 2018

## ABSTRACT

The wide deployment of Vehicle Automation and Communication Systems (VACS) in the following decade is expected to influence traffic performance on freeways. Apart from safety and comfort, one of the goals is the alleviation of traffic congestion that is a major and challenging problem for modern societies. This paper investigates the combined use of two feedback control strategies utilizing VACS in different penetration rates, aiming at maximising throughput at bottleneck locations. The first control strategy employs mainstream traffic flow control using appropriate variable speed limits as an actuator. The second control strategy delivers appropriate lane-changing actions to selected connected vehicles using a feedback-feedforward control law. Investigations of the proposed integrated scheme have been conducted using a microscopic simulation model for a hypothetical freeway featuring a lane-drop bottleneck. The produced results demonstrate significant improvements even for low penetration rates.

*Keywords*: traffic control, bottlenecks, variable speed limits, lane change control, connected vehicles

## INTRODUCTION

Freeway traffic congestion, typically initiated at bottleneck locations, is a major problem for modern societies, causing serious infrastructure degradation and underutilization especially during high-demand periods. Increased travel times, lower speeds and extended congestion in the network, are only a few of the immediate consequences. An efficient way to mitigate this problem is the development and implementation of proper traffic control strategies.

Bottleneck locations can be freeway merge areas, areas with a particular infrastructure layout (such as lane drops, strong grade or curvature, tunnels or bridges etc.), areas with specific traffic conditions (e.g. strong weaving of traffic streams) or areas with external capacity-reducing events (e.g. work-zones, incidents). If the arriving demand is higher than the bottlneck capacity, the bottleneck is activated, i.e. congestion is formed upstream of the bottleneck location. It should be emphasised, however, that, according to empirical investigations (*1*), capacity flow in conventional traffic is not reached simultaneously at all lanes. Thus, traffic breakdown may occur on one lane, while capacity reserves are still available on other lanes. This implies that the potentially achievable cross-lane capacity is not fully exploited. Naturally, once congestion appears on one lane, it spreads fast to the other lanes as well, as drivers on the affected lane attempt to escape the speed drop via lane changing. After congestion has occured, retarded and different vehicle acceleration at the congestion head causes the so-called capacity drop phenomenon, which breeds a reduction in the mainstream flow of a freeway, while congestion is forming upstream of the bottleneck location.

In the near future, Vehicle Automation and Communication Systems (VACS) are expected to revolutionise the features and capabilities of individual vehicles (*2*). The new features can be exploited via recommending, supporting, or even executing appropriately designed traffic control tasks. Vehicles equipped with VACS may act both as sensors (providing information on traffic conditions) and as actuators, permitting the deployment of strategies like Variable Speed Limits (VSL) (*3*) and Lane-Changing Control (LCC) (*4, 5*). Note that, while VSL control is also feasible by means of conventional control infrastructure, employing Variable Message Signs (VMSs), LCC is not feasible with conventional means, because it calls for the possibility to communicate with few individual vehicles, rather than with the whole vehicle population as by use of VMSs. Results from FHWA supported trials with cooperative vehicle-to-infrastructure systems can be found in (*6*).

Two feedback control strategies are investigated in combination in this study, aiming at mitigating congestion at bottlenecks. Specifically, LCC is used to achieve appropriate lane assignment of vehicles upstream of the bottleneck so as to increase the bottleneck capacity. On the other hand, Mainstream Traffic Flow Control (MTFC) via VSL guarantees that the flow approaching the bottleneck location is not exceeding the overall (possibly increased) capacity of the bottleneck. In order to test and evaluate the effectiveness of these strategies, four different scenarios are considered and ten replications are conducted for each scenario using a microscopic simulator for a lane-drop motorway infrastructure. To focus attention on the employed control methodologies, we assume full compliance of the connected vehicles and no communication delays with equipped vehicles. In the following, the detrimental effects of congestion at bottleneck locations are first discussed. Then, the feedback control strategies for MTFC via VSL and for LCC are outlined. The simulation setup is presented together with a discussion of the produced results. Finally, some conclusions are drawn.

## MOTORWAY BOTTLENECK ACTIVATION

Consider a hypothetical freeway stretch featuring a lane-drop bottleneck as in Figure 1 or any other kind of bottleneck mentioned above. As long as the arriving demand $q_{in}$ upstream of the bottleneck is less than or equal to the capacity $q_{cap}^{down}$ downstream of the bottleneck, no problem occurs. Congestion is initiated at bottleneck locations when the arriving demand $q_{in}$ is higher than the bottleneck capacity $q_{cap}^{down}$; then

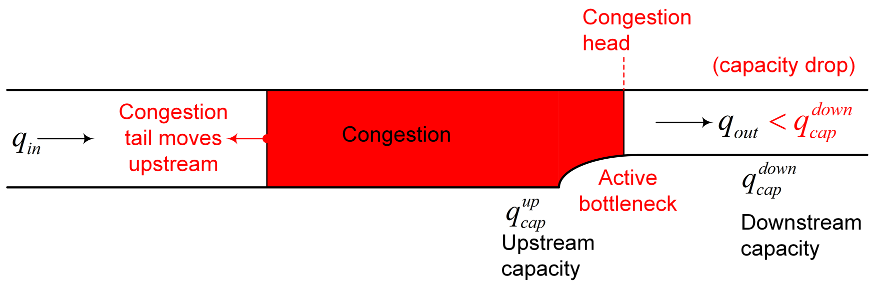


**FIGURE 1 The lane drop bottleneck notion**

the bottleneck is activated, i.e. congestion is created, which spills back covering areas upstream of the bottleneck location as long as the upstream arriving flow is sufficiently high. In these conditions, two kinds of detrimetnal effects have a major impact on freeway capacity and throughput (*7*):

- **Capacity drop (CD) at the congestion head:** Bottleneck activation leads to a speed breakdown at the bottleneck location. As a result, limited, different and retarded vehicle accelerations from lower (within the congestion) to higher speeds (downstream of the bottleneck), are deemed to lead to a capacity drop which breeds a reduction in the mainstream flow and consequently an active bottleneck outflow $q_{out}$ that may be 5% – 25% lower than the nominal capacity $q_{cap}^{down}$.

- **Blocking of off-ramps (BOR):** Congestion tail is covering ramps, as it moves upstream of the bottleneck location over several kilometers on the mainstream. As a result, the off-ramp flow drops as well, and vehicles bound for the off-ramps are getting trapped within the congestion, thus accelerating its spillback further upstream.

Note that the BOR effect is independent of the CD effect and leads to an additional reduction of the freeway throughput, i.e. it reflects an additional source of genuine infrastructure degradation (*7*).

## MAINSTREAM TRAFFIC FLOW CONTROL (MTFC)

VSL displayed on roadside or overhead VMS in response to prevailing traffic conditions is an increasingly popular freeway traffic control measure (*7*). A main targeted impact of VSL is enhanced traffic safety as a result of the homogenisation of speeds of individual vehicles and of the mean speeds of different freeway lanes which reduce the accident risk (*8*). In this work, VSL are applied to connected vehicles that may directly receive the value of the speed limit that is delivered by the control strategy, according to their current location in the network, and it is expected that, for sufficient penetration of equipped vehicles, this will be sufficient to impose the speed limit to non-equipped vehicles as well; hence, no VMS-gantries would be necessary.

The basic idea of MTFC is to enable the mainstream traffic flow approaching areas with particular infrastructure e.g. lane-drop or other bottlenecks, to take values ordered by an appropriate control strategy in order to establish optimal traffic conditions for any appearing demand (*9*). The MTFC concept used in this paper is illustrated in Figure 2. MTFC actions using VSL as an actuator are employed in order to regulate the mainstream flow upstream of the bottleneck location to be equal to the nominal capacity of the bottleneck $q_c \approx q_{cap}^{down}$. When MTFC actions are employed, a controlled congestion is formed further upstream of the bottleneck location leaving enough space for the vehicles to accelerate within the acceleration area and reach the bottleneck area with an increased speed. In this case, the capacity drop phenomenon is avoided, and thus

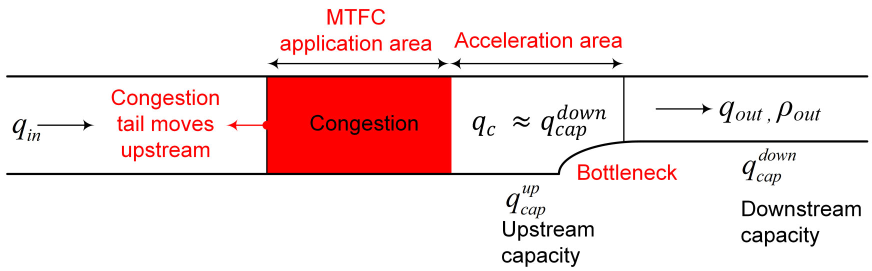


**FIGURE 2 The MTFC concept**

higher outflow is achieved. The controlled congestion is significantly reduced in space and time compared to the congestion created in the no-control case and has higher internal speeds due to the increased outflow values. This also leads to less blocking of off-ramps and hence further improvements on the freeway.

### MTFC Feedback Control Strategy

A Proportional - Integral (PI) feedback regulator is employed for MTFC, keeping the bottleneck density $\rho$ close to the selected set-point $\hat{\rho}$ using real time measurements (or estimates) of $\rho$ (*3*). The set-point is typically selected around the critical density value, at which capacity flow is achieved at the bottleneck location. The equation that describes the PI-type regulator reads:

$$vsl(k) = vsl(k-1) + K_I(\hat{\rho} - \rho(k)) + K_P(\rho(k-1) - \rho(k)) \tag{1}$$

with $k$ (=1,2,3,...) defined as the discrete time index. The time period T for updating decisions according to (1) is 60s. Proportional and Integral gains of the controller are denoted by $K_P$ and $K_I$, respectively. The $vsl(k)$ value delivered by the control strategy is truncated to remain within a range of admissible VSL values $[vsl_{min}, vsl_{max}]$ and the truncated value is used at the next time period as $vsl(k-1)$ in order to avoid the windup phenomenon (*10*). The VSL value is sent for application to all connected vehicles that are included in an MTFC application area of some 0.5km. Upstream of the MTFC application area (where VSL is active) there are VSL safety segments where speed limits are also applied to ensure a smooth reduction of speed and a safer vehicle approach to the application area. Furthermore, downstream of the application area, an acceleration area follows (see Figure 2) where an increased VSL is employed in order to allow a quick recovery of higher speeds by the vehicles so as to avoid the capacity drop and maximize the bottleneck throughput.

Some VSL practical implementation aspects are then taken into account. VSL obtained from (1) are rounded to the closest value of a set of predefined discrete values (e.g. 90, 80, 70,... km/h). Furthermore, the difference between two consecutive VSL values received by connected vehicles in a segment of the freeway is limited (e.g. to ±10 km/h), so as to avoid abrupt speed changes. Also, the difference between two VSL values at consecutive segments at the same control period is limited (e.g. to 10 km/h), as often required in practice, in order to achieve a safe approach of vehicles within the safety areas.

## LANE CHANGE CONTROL (LCC)

LCC is a promising new strategy that can be exploited for traffic management (*4, 5*). The basic goal of lane-changing control is to achieve a desired distribution of vehicles among the lanes in the immediate proximity of a bottleneck, so as to exploit the capacity of each and every lane, thus increasing the overall (cross-lane) capacity. To this end, a linear state-feedback control law, resulting from an appropriate linear-quadratic regulator problem formulation, is developed. The considered system under control comprises a number of interacting segment-lanes upstream of the bottleneck; while the feedback control law computes adequate lateral (lane-changing) flows for each segment-lane to be implemented by equipped vehicles, thus enabling an opportune, pre-specified distribution of traffic flow among the lanes. More specifically, the feedback control law uses real-time measurements (or estimates) of the state of the system, i.e. of all segment-lane densities, and is targeting appropriate pre-specified set-points of lane-based traffic densities.

## LCC Regulator Design

The problem of manipulating the lateral flows upstream of a bottleneck location in order to increase capacity and hence retard or avoid the creation of congestion, is formulated as a Linear Quadratic (LQ) optimal control problem. Based on a linear multi-lane traffic flow model proposed in (*4*), we consider a multi-lane freeway stretch subdivided into $i = 1, \ldots, N$ segments of length $L_i$, while each segment is composed of $j = m_i, \ldots, M_i$ lanes, where $m_i$ and $M_i$ are the minimum and maximum indexes of lanes for segment $i$. Each segment $i$ is composed of $M_i$ - $m_i$ + 1 cells; while each freeway cell is indexed by $(i, j)$. According to this definition, the total number of cells from the origin to segment $i$ is $H_i = \sum_{r=1}^{i}(M_r - m_r + 1)$. The total number of cells for the whole stretch is $\overline{H} = H_N$. It is assumed that $j = 1$ corresponds to the right most lane of the freeway. The model is formulated in discrete time, considering the discrete time step $T$ with a typical value of 10s. Each freeway cell $(i, j)$ illustrated in Figure 3 is characterized by traffic density, which is dynamically evolving following the conservation equation:

$$\rho_{i,j}(k+1) = \rho_{i,j}(k) + \frac{T}{L_i}\left[q_{i-1,j}(k) - q_{i,j}(k)\right] + \frac{T}{L_i}\left[f_{i,j-1}(k) - f_{i,j}(k)\right] + \frac{T}{L_i}d_{i,j}(k) \quad (2)$$

where:

- $\rho_{i,j}(k)$ is the density, i.e. the number of vehicles in cell $(i, j)$ at time $k$ divided by the segment length $L_i$ (veh/km),
- $q_{i,j}(k)$ is the longitudinal flow, i.e. the number of vehicles leaving segment $i$ and entering segment $i + 1$ remaining at lane $j$ during time interval $(k, k + 1]$ (veh/h),
- $f_{i,j}(k)$ is the lateral flow, i.e. the number of vehicles moving from lane $j$ to lane $j + 1$ during time interval $(k, k + 1]$ (veh/h) when positive, or the number of vehicles moving from lane $j + 1$ to lane $j$ during time interval $(k, k + 1]$ (veh/h) when negative,
- $d_{i,j}(k)$ is the external flow, i.e. the number of vehicles entering the network in cell $(i, j)$ during time interval $(k, k + 1]$ (veh/h).

Depending on the network topology, some terms of equation (2) may not be present for specific cells. Particularly, the inflow $q_{i-1,j}(k)$ does not exist for the first segment of the network; the outflow $q_{i,j}(k)$ does not exist for the last segment before a lane drop, while the lateral flow term $f_{i,j}(k)$ exists only for $m_i \leq j < M_i$. The external flow $d_{i,j}(k)$ exists only for a subset of cells (the upsteam-most in Figure 3). Consequently, following previous considerations the total number of lateral flows is $\overline{F} = \overline{H} - N$ (*5*).

Consider the well-known relationship:

$$q_{i,j}(k) = \rho_{ij}(k)v_{i,j}(k) \quad (3)$$

Using equation (3) and the conservation law equation (2), the following is obtained:

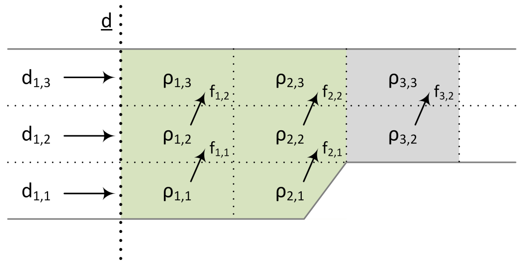


**FIGURE 3 Model formulation**

$$\rho_{i,j}(k+1) = \frac{T}{L_i} v_{i-1,j}(k)\rho_{i-1,j}(k) + \left[1 - \frac{T}{L_i} v_{i,j}(k)\right]\rho_{i,j}(k) + \frac{T}{L_i}\left[f_{i,j-1}(k) - f_{i,j}(k)\right] + \frac{T}{L_i} d_{ij}(k) \quad (4)$$

Treating speeds $v_{i,j}(k)$ as known parameters, a Linear Parameter Varying (LPV) system is obtained in the form:

$$\underline{x}(k+1) = A(k)\underline{x}(k) + B\underline{u}(k) + \underline{d}(k) \quad (5)$$

where we have the vectors of state, control and external disturbances, respectively, as follows:

$$\underline{x}(k) = \left[\rho_{1,m_1} \ldots \rho_{1,M_1} \quad \rho_{2,m_2} \ldots \rho_{N,M_N}\right]^T \in \mathbb{R}^{\overline{H}} \quad (6)$$

$$\underline{u}(k) = \left[f_{1,m_1} \ldots f_{1,(M_1-1)} \quad f_{2,m_2} \ldots f_{N,(M_N-1)}\right]^T \in \mathbb{R}^{\overline{F}} \quad (7)$$

$$\underline{d}(k) = \left[\frac{T}{L_1} d_{1,m_1} \ldots \frac{T}{L_1} d_{1,M_1} \quad \frac{T}{L_2} d_{2,m_2} \ldots \frac{T}{L_N} d_{N,M_N}\right]^T \in \mathbb{R}^{\overline{H}} \quad (8)$$

Matrix $A(k)$ reflecting the inter-connection between pairs of subsequent cells connected by a longitudinal flow $q_{i,j}(k)$ is composed of elements:

$$a_{r,s} = \begin{cases} 1, & \text{if } r = s \text{ and } (j < m_{i+1} \text{ or } j > M_{i+1}) \\ 1 - \frac{T}{L_i} v_{i,j}(k), & \text{if } r = s \text{ and } (i = N \text{ or } m_{i+1} \le j \le M_{i+1}) \\ \frac{T}{L_i} v_{i-1,j}(k), & \text{if } r > H_1 \text{ and } s = r - M_{i-1} + m_i - 1 \\ 0, & \text{otherwise} \end{cases}$$

Matrix $B$ reflecting the inter-connection of adjacent cells connected by lateral flows $f_{i,j}(k)$, is composed of elements:

$$b_{r,s} = \begin{cases} \frac{T}{L_i}, & \text{if } j > m_i \text{ and } s = r - i \\ -\frac{T}{L_i}, & \text{if } j < M_i \text{ and } s = r - i + 1 \\ 0, & \text{otherwise} \end{cases}$$

where $r = H_{i-1} + j + m_i + 1$.

Assuming that the inflow arriving upstream of the bottleneck location is not exceeding the maximum capacity of the bottleneck (e.g. thanks to MTFC measures), and hence any formation of congestion can be avoided, our system can be treated as a Linear Time Invariant (LTI) system. Specifically, in free flow conditions, it is assumed that speed $v_{i,j}(k)$ in all cells $(i, j)$ remains constant and equal to a speed value $v^*$ ($v_{i,j}(k) \equiv v^*$) close to the critical speed. Thus, matrix $A(k)$ is now treated as a constant matrix $A$. Also, external flows $d_{i,j}(k)$ are assumed constant to enable an LTI system and hence a time-invariant feedback controller. Note, however, that the external flows will be allowed to be time-varying according to measurements and will be explained later. The obtained LTI system reads:

$$\underline{x}(k + 1) = A\underline{x}(k) + B\underline{u}(k) + \underline{d} \tag{9}$$

In order to achieve a desired distribution of vehicles among the lanes downstream of the lane-drop area (see grey area in Figure 3), a quadratic cost function is defined, that penalises the difference between the cell densities at this area and pre-specified (constant) set-point values. A penalty term is also included aiming at maintaining small control inputs, i.e. small lateral flows (*4, 5*). The matrix form of the quadratic cost function reads:

$$J = \sum_{k=0}^{\infty} \left\{ \left[ C\underline{x}(k) - \underline{\hat{y}} \right]^T Q \left[ C\underline{x}(k) - \underline{\hat{y}} \right] + \underline{u}^T(k)\underline{u}(k) \right\} \tag{10}$$

where:

- $C$ is a matrix reflecting the cells that are tracked, (grey-area bottleneck cells)
- $Q$ is a weighting matrix associated to the magnitude of the state tracking error,
- $\underline{\hat{y}} \in \mathbb{R}^{\overline{Y}}$ is a vector containing the $\overline{Y}$ selected desired set-point density values at the bottleneck area.
- the time-horizon is infinite to enable a time-invariant feedback controller

Note that $Q = Q^T$ is a positive definite matrix and matrix C is composed of elemenets $c_{r,s}$ ($1 \leq r \leq \overline{Y}$ rows and $1 \leq s \leq \overline{H}$ columns). Each row of matrix C contains elements equal to zero and a single element equal to 1 that corresponds to the element of vector $\underline{x}$ that is tracked.

## LCC Linear State Feedback-Feedforward Control Law

The solution to the formulated optimal control problem is given through a Linear Quadratic Regulator (LQR) in the form of a linear state feedback-feedforward control law. To ensure a stabilizing feedback-feedforward control law, our system must be at least stabilisable and detectable, see (*4, 5*) for all the related details. The linear feedback-feedforward control law is given by:

$$\underline{u}^*(k) = -K\underline{x}(k) + \underline{u}_{ff} \tag{11}$$

where:

$$K = (I + B^T PB)^{-1} B^T PA \tag{12}$$

$$P = C^T QC + A^T PA - A^T PB(I + B^T PB)^{-1} B^T PA \tag{13}$$

$$\underline{u}_{ff} = (I + B^T PB)^{-1} B^T F(C^T Q\underline{\hat{y}} - P\underline{d}) \tag{14}$$

$$F = (I - (A - BK)^T)^{-1} \tag{15}$$

Note that the feedback gain matrix $K$ is calculated via (12) only once offline (time invariant controller) after solving the Ricatti equation (13) iteratively starting from $P = I$. Subsequently, equation (14) with $F$ from (15), represents the feedforward term that may be calculated offline. However, for practical implementation, one may measure the external flow $\underline{d}$, in which case the feedforward term becomes time-varying (online), with equations (11, 14) rewritten as:

$$\underline{u}^*(k) = -K\underline{x}(k) + \underline{u}_{ff}(k) \tag{16}$$

$$\underline{u}_{ff}(k) = \Phi - \Delta\underline{d}(k) \tag{17}$$

where $\Phi = (I + B^T PB)^{-1} B^T FC^T Q\underline{\hat{y}}$ and $\Delta = (I + B^T PB)^{-1} B^T FP$ may be calculated offline.

The LCC law delivers "macroscopic" lane-changing flows for each cell. These lateral flows are translated to corresponding vehicle numbers that should change lane in each cell, and related messages are submitted to a corresponding number of equipped vehicles. Note that the control design model is only used for deriving the LCC feedback law, which is robust, i.e. similarly efficient for changing speed values (corresponding to different "parameter" values in the control design model). Thus, although these assumptions of course do not hold true in a microscopic simulation model, the investigations reported in the following verify and demonstrate the effectiveness of the strategy with the controller being robust enough.

## SIMULATION INVESTIGATIONS

### Network Description

A hypothetical freeway stretch featuring a lane-drop bottleneck is considered in this paper for investigating the integrated use of the two feedback control strategies. Four scenarios are defined (no-control scenario, variable speed limits scenario, lane changing control scenario, integrated control scenario). The freeway stretch illustrated in Figure 4 consists of 10 segments of 0.5 km each, resulting in a total 5.0 km length. The biggest part of the network features 3 lanes starting from the entrance until reaching the 4.0 kilometer of the freeway where the right-most lane (lane 1) drops, after which the last kilometer has 2 lanes. Lane 2 is the middle lane and lane 3 is the left lane of the network (fast lane). When no VSL values are applied, the nominal speed limit is 100 km/h for all sections except for the two consecutive segments upstream of the bottleneck where the speed limit is 80 km/h.

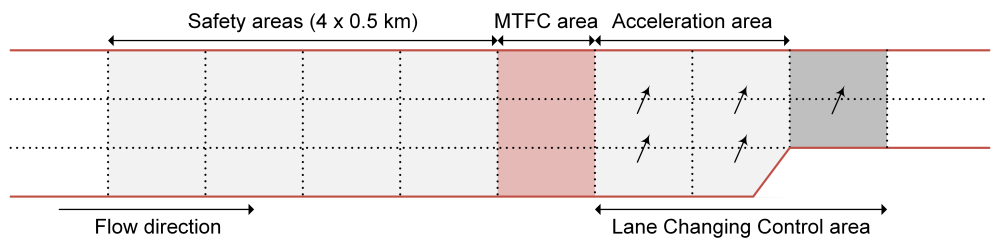


**FIGURE 4 Freeway stretch used is simulations with the corresponding strategies**

## Configuration of the microscopic model

The infrastructure layout for the investigation of the proposed strategies was developed and tested using Aimsun Microscopic Simulator (*11*). AIMSUN includes the AAPI and the microSDK tools, that allow the replacement of the default models used by the simulator. The MTFC and the LCC strategies were implemented using the AAPI tool; while the microSDK tool was used to overwrite Aimsun's default behavioral models.

The MTFC strategy utilizes density measurements aggregated over lanes for the lane-drop area and produces as an output the VSL values to be applied in the MTFC application area by all equipped vehicles in that area. Full compliance is assumed. The LCC strategy utilizes segment-lane density measurements for all cells in the controlled area as well as measurements of the external demand per lane in order to produce as an output the lateral flows to be implemented by a corresponding number of equipped vehicles within each segment-lane. In case of low penetration rates it may be necessary to use all equipped vehicles within a segment-lane, while in high penetration rates it may be enough to use just some of them that are picked randomly. Note that some ordered lane changes may not materialise, because they would violate some safety conditions set by the simulator. This leads factually to a limited "compliance" to the LCC commands, whose impact, however is largerly rejected thanks to the feedback nature of the controller. In all cases, non-equipped vehicles are allowed to change lanes as usual, and their actions are just a disturbance for the LCC controller, which is however rejected thanks to the feedback nature of the regulator used.

Aimsun uses the Gipps Car Following Model (*12*) to represent the movement of vehicles. However, this model does not reproduce the capacity drop phenomena in critical regimes (*13*), and, for this reason, it was replaced with the Intelligent Driver Model (IDM) car-following model (*14*), which reflects significant aspects of the traffic flow dynamics and features crash-free collective dynamics (*15*). In relation to lateral movements, Aimsun uses the Gipps Lane Changing Model (*16*). The main limitation of this model is that it cannot capture realistically the merging behavior in a critical flow regime (*17*), and therefore it is complemented at critical merging locations (i.e. bottleneck area) with the addition of some heuristic rules (*18*) while for the rest of the freeway, the original Gipps model is used. Ten replications are conducted for each scenario for a simulation horizon of 60 min. Each replication has the same average demand profile and the same mean values for all vehicle-related parameters. For each scenario, one replication close to the average of the ten replications is selected for presentation in the following sections. The traffic demand profile for one of the replications is depicted in Figure 5. It can be observed that the demand is increasing for about 10 minutes reaching values (~4200 veh/h) well above the capacity of the bottleneck (3600 veh/h). The demand remains high for about 15 minutes and then it is decreasing and is staying at low values so as to allow for free flowing conditions at the end of the simulation horizon for all scenarios considered and, as a result, allow also the comparison of performance indexes between different scenarios.

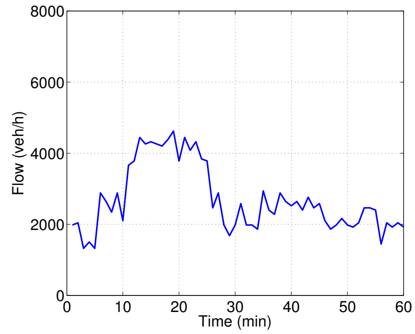


**FIGURE 5 Traffic demand profile**

## Simulation Results

*No-Control Scenario*

In the no-control scenario congestion starts at $t = 16$ min, as the arriving demand exceeds capacity, and lasts for about 30 min. It spills back covering several sections (1.5 km) upstream of the bottleneck location as depicted in the speed contour plot presented in Figure 6(a). Density trajectories are displayed in Figure 6(b) for each lane at the lane-drop area. After $t = 16$ min a quasi-simultaneous steep rise of density at lanes 2 and 3 indicates the corresponding drop of speeds and the formation of congestion at all lanes. A capacity drop of about 14% of the nominal capacity of the bottleneck is observed in Figure 6(c). The outflows per lane, displayed in Figure 6(d), validate that lane 2 (blue trajectory) reaches its capacity ($\approx 2100$ veh/h), after which speed breaks down, and congestion spreads immediately to lane 3 (red trajectory) that also breaks down at 1700 veh/h, i.e. before reaching its capacity. The average Total Travel Time (TTT) value for the no-control scenario is 223.3 veh·h.

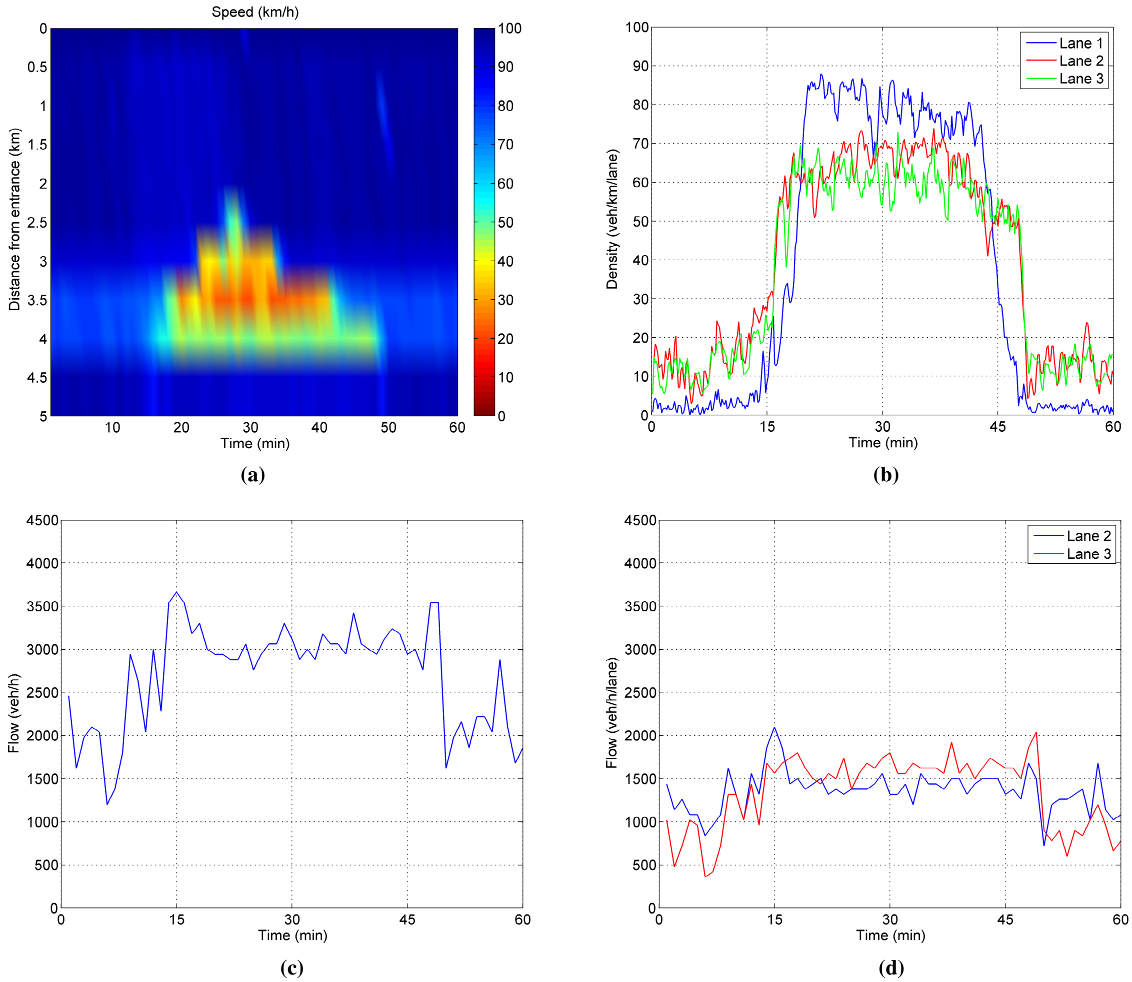


**FIGURE 6 (a) Speed contour plot; (b) per lane density trajectories; (c) total outflow trajectory; and (d) per lane outflow trajectories at the lane-drop area for the no-control scenario**

### *Variable Speed Limits Scenario*

The main goal of MTFC is to regulate the mainstream flow upstream of the bottleneck, i.e. at the MTFC application area indicated in Figure 4, in order to maximise throughput. The penetration rate of connected vehicles that receive and apply VSL values is initially set to 20%. The speed contour plot resulting from MTFC application in the present investigation is presented in Figure 7(a). All actions are delivered by the PI controller (1) every 60 sec with a set-point equal to the critical density of 25 veh/km/lane, for which capacity flow is reached at the no-control scenario. Minimum and maximum values of VSL are set to 20 km/h and 100 km/h, respectively. No MTFC action is necessary up to $t = 16$ min. Then, as illustrated in Figure 7(b), density at the bottleneck area (lane-drop area) is increasing approaching the set-point. Therefore, VSL values ordered by (1) are gradually decreasing, reaching the minimum admissible value (Figure 7(b)). All practical implementation aspects mentioned below (1) are applied.

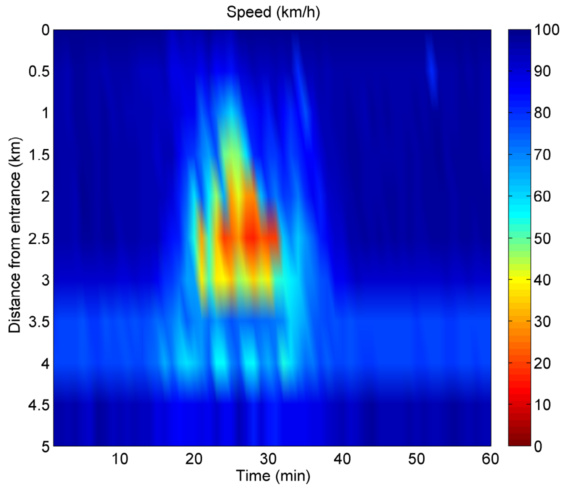


**(a)**

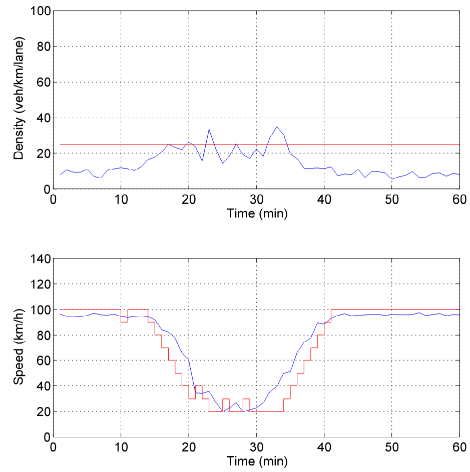


**(b)**

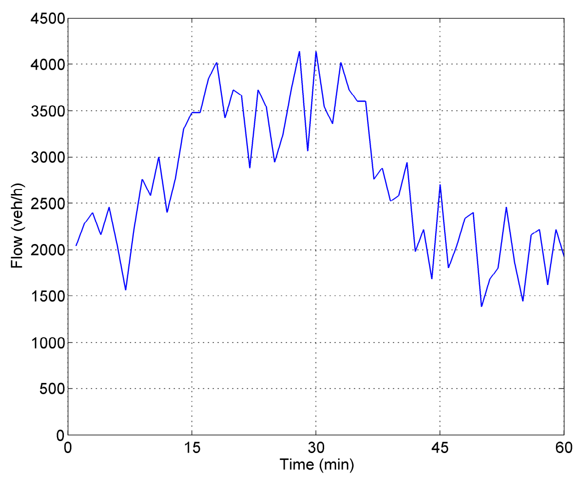


**(c)**

**FIGURE 7 (a) Speed contour plot; (b) density measurements (blue line) at the bottleneck area (lane-drop area) with the corresponding critical density value (red line) and speed measurements at the MTFC application area with the corresponding speed limits (red line); and (c) total outflow trajectory at the lane-drop area for the VSL scenario**

Density at the bottleneck area (lane-drop area) is maintained around the set-point. Speed measurements at the MTFC application area demonstrate that a penetration rate of 20% is sufficient to drive the average speed of all vehicles close to the ordered VSL value. Due to VSL actions, a controlled congestion is formed further upstream, that is reduced in space and time compared to the one formed in the no-control scenario. An improvement of 6.4% is achieved on the average TTT value. As observed in Figure 7(c), capacity drop is now avoided at the lane-drop area. Some low-pick values marked between the 20th and the 30th minute of the simulation are due to undershooting of density (see also Figure 7(b)).

As demonstrated in Figure 8, higher values in penetration rate of connected vehicles result in higher achieved improvement of the average TTT value, approaching the value that corresponds to the case of VSL values displayed on VMS gantries, which corresponds to 100% penetration.

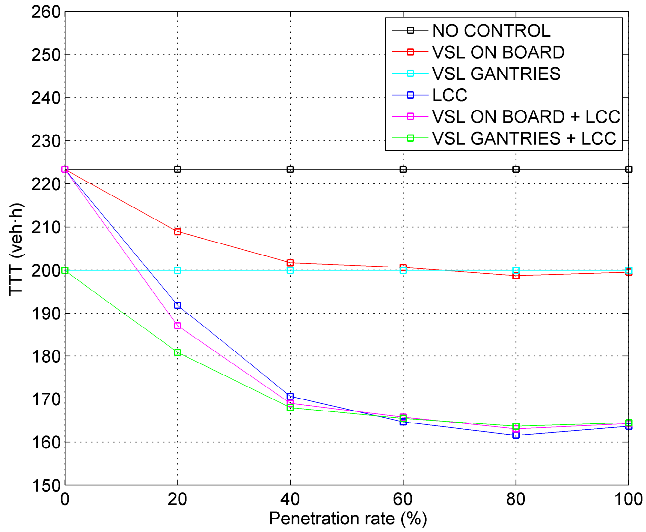


**FIGURE 8 Average Total Travel Time (TTT) per penetration rate of connected vehicles for the no-control case and control cases**

*Lane Change Control Scenario*

In this scenario, the goal of the controller is to achieve a density distribution at the area downstream of the lane drop that allows the full exploitation of capacity of each lane. This is done by delivering appropriate lateral flows by the linear feedback-feedforward control law (16) every 10 sec. Speed contour plots resulting from the LCC application at the present investigation are provided in Figure 9. The set-points used are 28 veh/km/lane for lane 2 and 33 veh/km/lane for lane 3 downstream of the lane-drop area.

For a penetration rate of connected vehicles equal to 20% it can be seen from Figure 10(a) (when also compared with Figure 6(d)) that a higher outflow is achieved for lane 3 and that both lane 2 and lane 3 have a capacity around 2100 veh/h that is maintained for about 8 min. However, the lateral flows ordered by LCC cannot be fully realized and the goal of the controller is not achieved for lane 3 (see Figure 11(a)). Congestion is then created due to further increasing demand, a capacity drop appears, and spillback of the congestion covers almost 1 km upstream of the lane drop area. Nevertheless, a 14.6% improvement of the average TTT is obtained compared to the no-control case. As observed in Figure 8, the achieved improvement in TTT increases for higher penetration rates reaching 27%.

For a penetration rate of connected vehicles equal to 80%, it can be observed (Figure 10(b)) that even higher outflow values can be achieved for lane 3. This is because the lateral flows ordered by LCC can be realized, and the goal of the controller is virtually achieved for a long period of time (see also Figure 11(b)). No congestion is created due to higher capacity values. The flow drop observed at $t$ = 30 min is due to a decrease of the demand. It should be noted, however, that an even higher demand could lead to a break down even in case of high penetration rates if only LCC is applied, because LCC aims at increasing the bottleneck capacity, but it cannot prevent congestion if the arriving demand increases beyond the increased capacity.

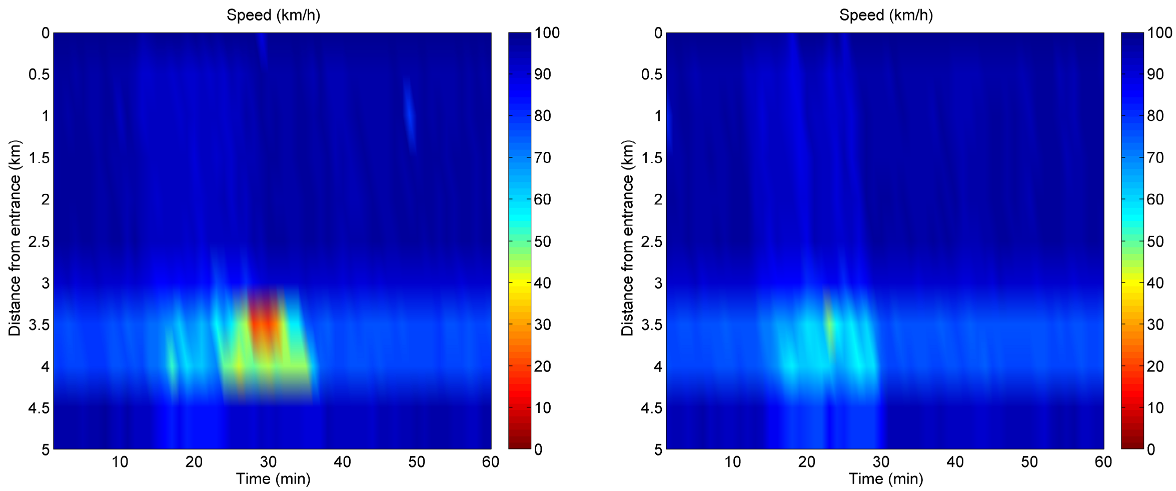


(a) (b)

**FIGURE 9 Speed contour plots for (a) 20% and (b) 80% of connected vehicles respectively for the LCC scenario**

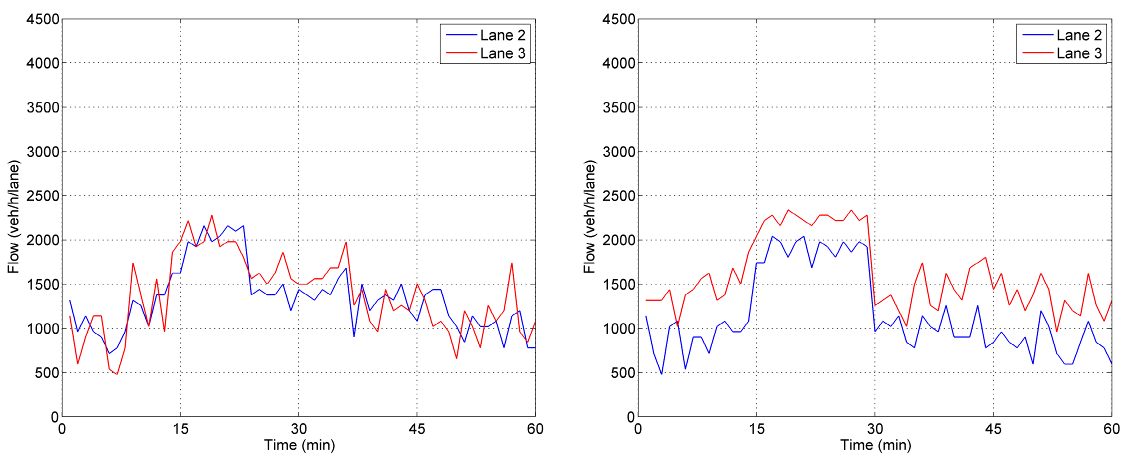


(a) (b)

**FIGURE 10 Per lane outflow trajectories at the bottleneck area (lane-drop area) for (a) 20% and (b) 80% of connected vehicles respectively for the LCC scenario**

## *Integrated Control Scenario*

In this case, MTFC is applied in addition to LCC to ensure that no congestion is created at the bottleneck and that the increased capacity due to LCC actions is maintained for longer periods of time. Speed contour plots are provided in Figure 12. Due to the increased capacity, higher set-points (35 veh/km/lane) are used in (1) for the density values. For a penetration rate of connected vehicles equal to 20%, there is an increased improvement compared to both previous non-integrated scenarios. As observed in Figure 13(a), VSL actions are still strong, without however reaching the minimum admissible value of 20 km/h.

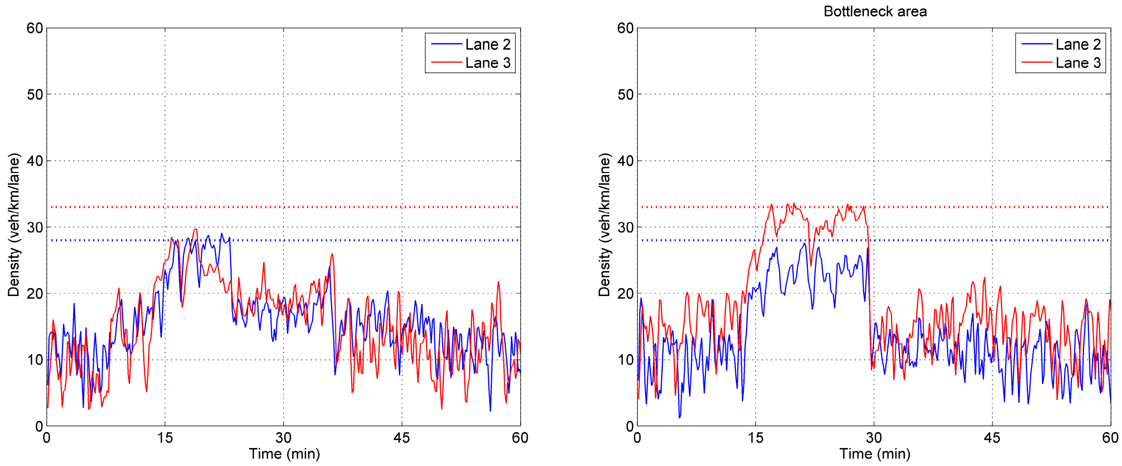


(a) (b)

**FIGURE 11 Per lane density trajectories (continuous lines) and corresponding set-points (dotted lines) downstream of the bottleneck area (lane-drop area) for (a) 20% and (b) 80% of connected vehicles for the LCC scenario**

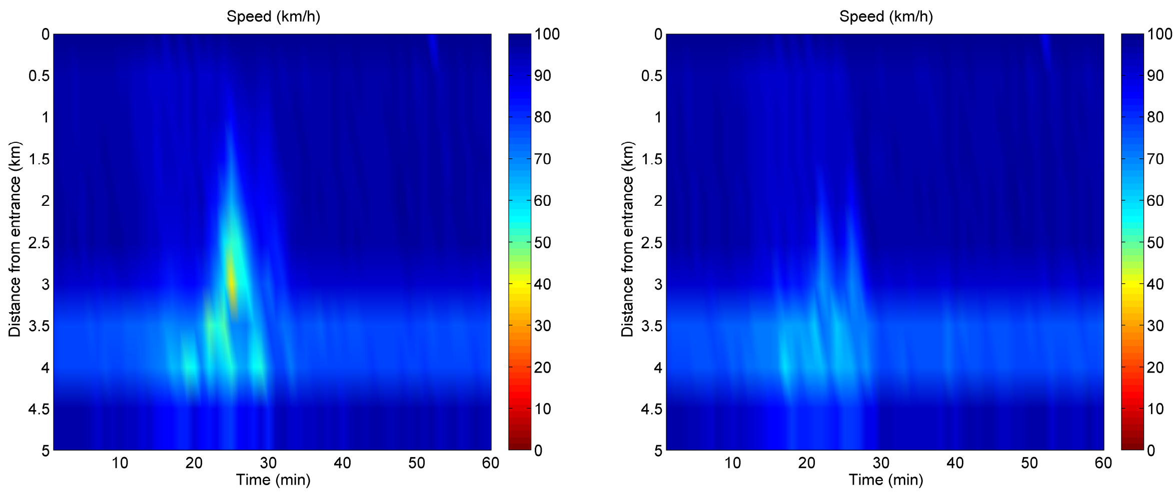


(a) (b)

**FIGURE 12 Speed contour plots for (a) 20% and (b) 80% of connected vehicles respectively for the integrated control scenario**

For a penetration rate of connected vehicles equal to 80%, VSL actions are moderate (Figure 13(b)) and TTT values are virtually equal to the ones obtained for the corresponding LCC scenario (see Figure 8).

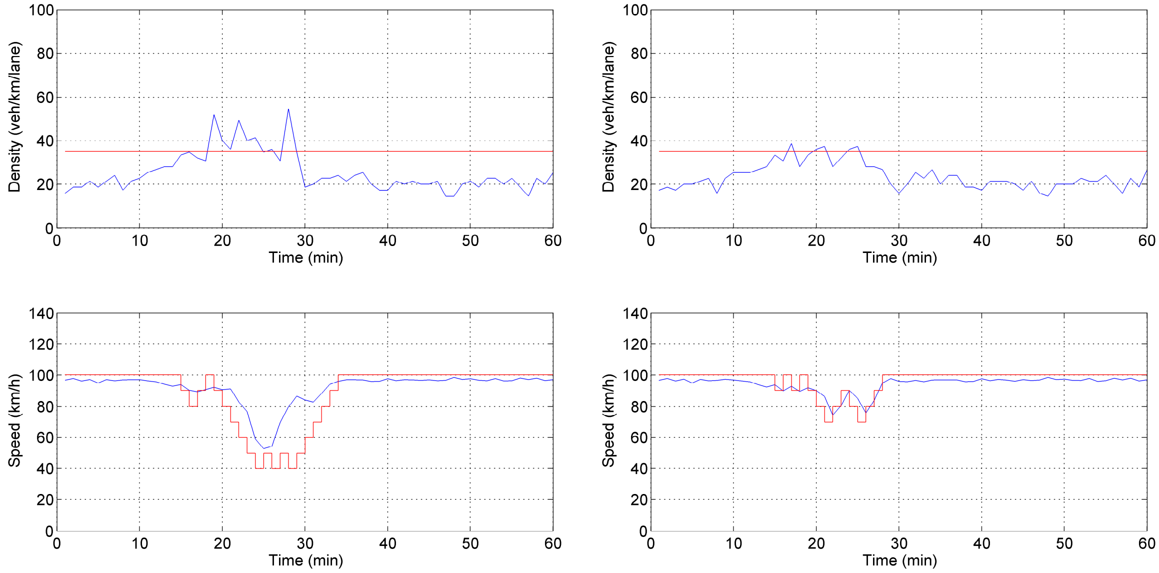


**(a)** **(b)**

**FIGURE 13 Density measurements (blue line) at the bottleneck area (lane-drop area) with the corresponding critical density value (red line) and speed measurements at the MTFC application area with the corresponding speed limits (red line) for (a) 20% and (b) 80% of connected vehicles for the integrated control scenario**

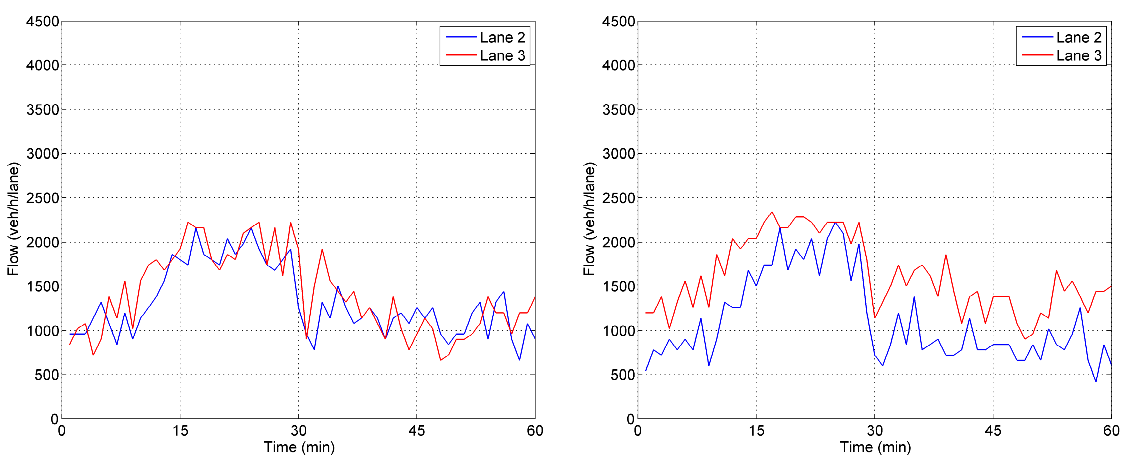


**(a)** **(b)**

**FIGURE 14 Per lane outflow trajectories at the bottleneck area for (a) 20% and (b) 80% of connected vehicles respectively for the integrated control scenario**

Figure 14(a) demonstrates that for a penetration rate of 20% the increased capacity achieved for lane 3 is maintained for a longer period of time compared to the non-integrated (LCC only) scenario (see also Figure 10(a)). For a penetration rate of 80% the capacity values achieved (Figure 14(b)) are similar to the non-integrated LCC scenario (Figure 10(b)).

## CONCLUSION

This paper presented the combined deployment and evaluation of previously proposed control strategies, namely the MTFC via VSL and the LCC, using a microscopic simulation model for a lane-drop infrastructure. VSL, even for low penetration rates, have been proven successful in avoiding the capacity drop. LCC is able to achieve an appropriate lane assignment of vehicles upstream of the bottleneck and as a result increase its capacity. For low penetration rates of connected vehicles the integrated use of the two strategies is demonstrated to be highly beneficial. The reported results were obtained assuming full compliance and no communication delays. In the frame of the EU H2020 project INFRAMIX (https://www.inframix.eu/), we plan to investigate issues related to partial relaxing of such assumptions, utilizing more realistic models for connected and automated vehicles, related communications, etc., for some more bottleneck types and infrastructure layouts. Within the same project, we also plan to test some aspects of the presented concepts in real field tests.

## ACKNOWLEDGEMENTS

The research leading to these results has received funding partially from the European Research Council under the European Union's Seventh Framework Programme (FP/2007-2013) / ERC Grant Agreement no 321132, project TRAMAN21 and partially from the European Union's Horizon 2020 research and innovation programme under grant agreement no 723016, project INFRAMIX. Content reflects only the authors' view. The Innovation and Networks Executive Agency (INEA) is not responsible for any use that may be made of the information it contains. The authors would like to thank all partners within INFRAMIX for their cooperation and valuable contribution.

## REFERENCES


1. Knoop, V. L., A. Duret, C. Buisson, and B. Van Arem, Lane distribution of traffic near merging zones influence of variable speed limits. In *Proceedings of the 13th International IEEE Conference on Intelligent Transportation Systems*, 2010, pp. 485–490.
2. Diakaki, C., M. Papageorgiou, I. Papamichail, and I. Nikolos, Overview and analysis of vehicle automation and communication systems from a motorway traffic management perspective. *Transportation Research Part A: Policy and Practice*, Vol. 75, 2015, pp. 147–165.
3. Carlson, R. C., I. Papamichail, and M. Papageorgiou, Comparison of local feedback controllers for the mainstream traffic flow on freeways using variable speed limits. *Journal of Intelligent Transportation Systems*, Vol. 17, No. 4, 2013, pp. 268–281.
4. Roncoli, C., N. Bekiaris-Liberis, and M. Papageorgiou, Optimal lane-changing control at motorway bottlenecks. In *Intelligent Transportation Systems (ITSC), 2016 IEEE 19th International Conference on*, IEEE, 2016, pp. 1785–1791.
5. Roncoli, C., N. Bekiaris-Liberis, and M. Papageorgiou, Lane-changing feedback control for efficient lane assignment at motorway bottlenecks. *Transportation Research Record: Journal of the Transportation Research Board*, Vol. 2625, 2017, pp. 20–31.
6. Hale, D., T. Phillips, K. Raboy, J. Ma, P. Su, X.-Y. Lu, H. Rakha, D. J. Dailey, et al., *Introduction of cooperative vehicle-to-infrastructure systems to improve speed harmonization*. United States. Federal Highway Administration. Office of Operations Research and Development, 2016.
7. Carlson, R. C., I. Papamichail, M. Papageorgiou, and A. Messmer, Optimal motorway traffic flow control involving variable speed limits and ramp metering. *Transportation Science*, Vol. 44, No. 2, 2010, pp. 238–253.
8. Papageorgiou, M., E. Kosmatopoulos, and I. Papamichail, Effects of variable speed limits on motorway traffic flow. *Transportation Research Record: Journal of the Transportation Research Board*, Vol. 2047, 2008, pp. 37–48.
9. Carlson, R. C., I. Papamichail, M. Papageorgiou, and A. Messmer, Optimal mainstream traffic flow control of large-scale motorway networks. *Transportation Research Part C: Emerging Technologies*, Vol. 18, No. 2, 2010, pp. 193–212.
10. Shinskey, F., Process control systems: application, design, and tuning. McGraw-Hill Co. *Inc., New York, NY*, 1996.
11. Systems, T. S., *Aimsun Dynamic Simulators User's Manual*. 8th ed., 2013.
12. Gipps, P. G., A behavioural car-following model for computer simulation. *Transportation Research Part B: Methodological*, Vol. 15, No. 2, 1981, pp. 105–111.
13. Wang, J., R. Liu, and F. Montgomery, Car-following model for motorway traffic. *Transportation Research Record: Journal of the Transportation Research Board*, Vol. 1934, 2005, pp. 33–42.
14. Treiber, M., A. Hennecke, and D. Helbing, Congested traffic states in empirical observations and microscopic simulations. *Physical review E*, Vol. 62, No. 2, 2000, pp. 1805–1824.
15. Kesting, A., M. Treiber, and D. Helbing, Enhanced intelligent driver model to access the impact of driving strategies on traffic capacity. *Philosophical Transactions of the Royal Society of London A: Mathematical, Physical and Engineering Sciences*, Vol. 368, No. 1928, 2010, pp. 4585–4605.
16. Gipps, P. G., A model for the structure of lane-changing decisions. *Transportation Research Part B: Methodological*, Vol. 20, No. 5, 1986, pp. 403–414.
17. Chevallier, E. and L. Leclercq, Do microscopic merging models reproduce the observed priority sharing ratio in congestion? *Transportation Research Part C: Emerging Technologies*, Vol. 17, No. 3, 2009, pp. 328–336.

18. Roncoli, C., I. Papamichail, and M. Papageorgiou, Model predictive control for multi-lane motorways in presence of VACS. In *Intelligent Transportation Systems (ITSC), 2014 IEEE 17th International Conference on*, IEEE, 2014, pp. 501–507.